A model-based Bayesian framework for ECG beat segmentation

2009 Physiol. Meas. 30 335

(http://iopscience.iop.org/0967-3334/30/3/008)

IOP PUBLISHING PHYSIOLOGICAL MEASUREMENT

Physiol. Meas. **30** (2009) 335–352 doi:10.1088/0967-3334/30/3/008

A model-based Bayesian framework for ECG beat segmentation

O Sayadi and M B Shamsollahi

Biomedical Signal and Image Processing Laboratory (BiSIPL), School of Electrical Engineering, Sharif University of Technology, Tehran, Iran

E-mail: osayadi@ee.sharif.edu and mbshams@sharif.edu

Received 13 November 2008, accepted for publication 23 January 2009
Published 25 February 2009
Online at stacks.iop.org/PM/30/335

Abstract

The study of electrocardiogram (ECG) waveform amplitudes, timings and patterns has been the subject of intense research, for it provides a deep insight into the diagnostic features of the heart's functionality. In some recent works, a Bayesian filtering paradigm has been proposed for denoising and compression of ECG signals. In this paper, it is shown that this framework may be effectively used for ECG beat segmentation and extraction of fiducial points. Analytic expressions for the determination of points and intervals are derived and evaluated on various real ECG signals. Simulation results show that the method can contribute to and enhance the clinical ECG beat segmentation performance.

Keywords: correction algorithm, ECG dynamical model, extended Kalman filter, fluctuating estimates, fiducial points extraction, segmentation

(Some figures in this article are in colour only in the electronic version)

1. Introduction

Automatic analysis of the electrocardiogram (ECG) has been the subject of intense research during the last three decades and is well known in the physiological measurement field. The particular interest for ECG analysis comes from its role as an efficient noninvasive investigative method which provides useful information for the detection, diagnosis and treatment of cardiac diseases. The ECG signal has a time pseudo-periodicity allowing for the definition of an elementary beat composed of specific waveforms PQRST, appearing pseudo-periodically in time. Each individual heartbeat comprises a number of distinct cardiological stages, which in turn give rise to a set of distinct features in the ECG waveform. These features represent either depolarization (electrical discharging) or repolarization (electrical recharging) of the muscle cells in particular regions of the heart. The standard features of the ECG waveform are the

P wave, the QRS complex and the T wave. Additionally a small U wave is occasionally present, which does not contain significant diagnostic information. The cardiac cycle begins with the P wave (the start and end points of which are referred to as P_{on} and P_{off}), which corresponds to the period of atrial depolarization in the heart. This is followed by the QRS complex, which is generally the most recognizable feature of an ECG waveform, and corresponds to the period of ventricular depolarization. The T wave follows the QRS complex and corresponds to the period of ventricular repolarization. The end point of the T wave is referred to as T_{off} and represents the end of the cardiac cycle (presuming the absence of a U wave). Moreover, the timing between the onset and offset of particular features of the ECG, which is being referred to as an interval, is of great importance since it provides a measure of the state of the heart and can indicate the presence of certain cardiological conditions (Clifford *et al* 2006).

The general aim of any signal segmentation method is to 'partition' a given signal into consecutive regions of interest. In the context of the ECG then, the role of segmentation is to determine as accurately as possible the onset and offset boundaries, as well as the peak locations, of the various waveform features, such that the ECG interval measurements may be computed automatically and the study of waveform patterns will be facilitated. For instance, one can easily show that the heart rate is estimated after detecting the QRS complex from a beat sequence. In the same way, the time distance between two consecutive QRS complexes, known as the RR interval, is used to detect premature beats. This analysis may be extended to other conditions like the ST-segment deviation from a long period, necessary to early diagnosis of ischemia. As a result, reliable ECG analysis depends directly on the ECG beat segmentation results (Kadish 2001).

The focus of this paper is to segment a given ECG, which in turn requires the detection of the fiducial points (FPs) and the peak locations related to the five main waveforms. FPs in an ECG signal are the onset and offset of P and T waveforms, the locations of QRS complex and the peak which is the extremum of the characteristic waves.

Efforts have been aimed at coping with the problem of extraction of characteristic points in an ECG. Most works in this field employ heuristic rules to segment heartbeat automatically from the ECG signal after performing a suitable preprocessing technique (Gritzali *et al* 1989, Laguna *et al* 1994, Li *et al* 1995, Vullings *et al* 1998, Köhler *et al* 2002), and many authors underline the advantages of the wavelet transform (Li *et al* 1995, Afonso *et al* 1999, Kadambe *et al* 1999, Mahmoodabadi *et al* 2005, Krimi *et al* 2006). The multiscale decomposition improves robustness, when the signal is corrupted by noise (Köhler *et al* 2002). On the other hand, regarding the beat classification task, a large number of methods have already been proposed. In general, the classification approaches are heuristic, namely decision trees and fuzzy logic (Kors and Bemmel 1990), and statistics, namely discriminant analysis (Kors and Bemmel 1990), hidden Markov models (Coast *et al* 1990), neural networks (Bortolan *et al* 1990, Hu *et al* 1997, Andreão *et al* 2002) and statistical rule-based systems (Elghazzawi and Gehed 1996).

Recently, Bayesian filters such as the extended Kalman filter (EKF) were proposed for ECG denoising (Sameni *et al* 2007). The state-space model (SSM) used in these approaches was inspired from the work by McSharry *et al* (2003), which suggested the use of Gaussian mixture models to generate realistic synthetic ECGs. It was later found that by simple modifications, the ECG filtering framework developed by Sameni *et al* (2007) could be used as a general framework for model-based ECG filtering (Sayadi *et al* 2007), simultaneous denoising and compression (Sayadi and Shamsollahi 2008a) and filtering cardiac contaminants (Sameni *et al* 2008).

In this paper, we take advantage of the estimations provided by the modified framework (Sayadi and Shamsollahi 2008a) to fully determine the locations of characteristic waveforms

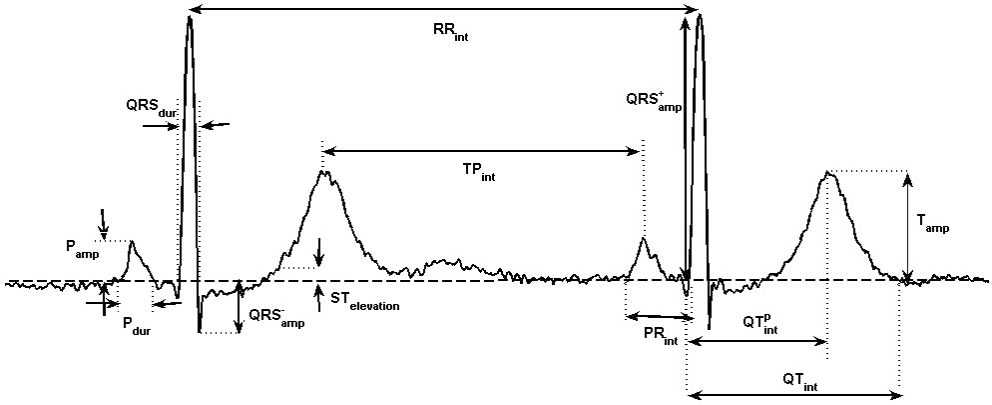

Figure 1. Single-beat and multiple-beat morphological features of a typical ECG signal.

and their corresponding FPs. We also present the details of this general framework for beat-to-beat segmentation and interval representation. Moreover, several examples are presented and the method is compared to some benchmark algorithms.

The paper is organized as follows. In section 2, the basic model-based idea for ECG beat segmentation is presented. In section 3, the previously developed Bayesian framework for estimating the required parameters for segmentation is reviewed. The details of the proposed extension and analytic derivations using the EKF structure are presented in section 4. Section 5 is devoted to simulation results. Finally, discussion and concluding remarks are provided in section 6.

2. Model-based ECG beat segmentation

According to the previous definition, ECG beat segmentation is the process of extracting multiple points in the signal so that not only successive beats are separated but also the waveforms embedded in every single beat are being distinguished. This definition clarifies two types of morphological features in an ECG signal; single-beat and multiple-beat features. The former points to those features that are extracted from a single beat on an ECG signal, such as the amplitudes of P, Q, R, S and T, or the P, QRS and T duration. Meanwhile, the latter refers to the features that are dependent to at least two successive beats, such as the RR or TP interval. Typical morphologic features of ECG waveforms and the corresponding time intervals are illustrated in figure 1. As can be seen, the majority of shown features depend directly on determination of the locations of FPs and the peak points, which are generally regarded as the segment symbols.

Simple investigation of figure 1 implies that we need to locate the beginning, the peak and the end point of PQRST waveforms to obtain the shape features. The detection of the QRS complex is the most important task, since it provides a more detailed examination of ECG signal, including beat separation, the heart rate, the ST segment, etc. Most of the QRS detectors are based on decision rules and thresholding of a filtered and transformed version of the signal, which suffer from three problems: (1) variations of the QRS frequency band for different subjects, (2) overlaps between the frequency content of QRS and noise and (3) dependence of the threshold value on the signal (Köhler *et al* 2002).

The same story is true for P and T waves. The P waves are usually a low-amplitude feature that can often become subsumed by the baseline noise in a signal. The enormity of this problem has led to a pervasive analysis of beat-to-beat intervals based upon the QRS complex as a fiducial marker, including the syntactic method (Skordalakis 1986) and the hidden Markov method (Coast *et al* 1990), which are complex and time-consuming, length transformation for *P* and *T* detection (Gritzali *et al* 1989) and the application of wavelet transform for the T wave detection (Krimi *et al* 2006).

A simple interpretation for the determination of the segment symbols is to model every heartbeat as a combination of finite kernels, such as Gaussian kernels. In other words, if we assume that every beat of an ECG signal can comprise finite Gaussian kernels, then the parameters of these kernels can be related to the fiducial and peak points. However, the exact relation between the kernel variables and the segment symbols are not derived so far. Hence, as a pioneer work for the purpose of beat segmentation, we consider a combination of five Gaussian kernels to represent a single ECG cycle, so that each kernel stands for one of the PQRST waveforms. This idea originates from the synthetic model that was proposed for generating artificial ECGs, which unifies the morphology and pulse timing in a single nonlinear dynamic model (McSharry *et al* 2003). The model generates a three-dimensional trajectory which consists of a circular limit cycle in the polar plane that is pushed up and down as it approaches each of the wave centers, as shown in figure 2(a). The simplified discrete version of the model is shown as

$$\begin{cases} \varphi_{k+1} = \varphi_k + \omega \cdot \delta \\ s_{k+1} = s_k - \displaystyle\sum_{i \in \{P,Q,R,S,T\}} \delta \cdot \frac{\alpha_{i_k}\omega}{b_{i_k}^2} \cdot \Delta\theta_i[k] \exp\left(-\frac{\Delta\theta_{i_k}^2}{2b_{i_k}^2}\right) + \eta, \end{cases} \tag{1}$$

where δ is the sampling period, $\omega = 2\pi f$, f is the beat-to-beat heart rate and $\Delta\theta_{i_k} = (\varphi_k - \theta_{i_k}) \bmod(2\pi)$. φ is a saw-tooth-shape signal that is expected to be zero at R-peaks, and being linearly assigned a phase between $-\pi$ and π to the ECG samples between two successive R-peaks (figure 2(b)). α_i, b_i and θ_i are the amplitude, angular spread and location of the Gaussian functions, respectively, and η is a random additive white noise which represents the baseline wander effects and models other additive sources of process noise. Concerning the simplicity and flexibility of this model, it can be easily used as a base for ECG processing, as demonstrated by Clifford *et al* (2005), where the use of the model to filter, compress and classify the ECG was first proposed.

Prior to the derivation of analytic formulas for the extraction of segment symbols, it is necessary to be more familiar with the characteristic parameters of a Gaussian kernel (GK). A general GK is written in the following form:

$$y_{\mathrm{GK}} = A \exp\left(-\frac{(x_{\mathrm{GK}} - \mu)^2}{\sigma^2}\right), \tag{2}$$

where A, μ and σ determine the amplitude, center and spread of the function y, respectively. It can be assumed that the ECG waveform peaks correspond to the center parameters of Gaussian functions, where the trajectory reaches to its local maxima/minima. This way, the θ_i parameter, which stands for μ, determines the PQRST peak locations as follows:

$$\begin{aligned} P_{\mathrm{peak}} &= \theta_P, \qquad Q_{\mathrm{peak}} = \theta_Q, \qquad R_{\mathrm{peak}} = \theta_R, \\ S_{\mathrm{peak}} &= \theta_S, \qquad T_{\mathrm{peak}} = \theta_T. \end{aligned} \tag{3}$$

The center positions for a typical synthetic trajectory are shown in figure 2(a) with small filled circles. In order to find the onset and offset of the waveforms, we have taken advantage of the spread parameter. Hence, to determine the onset and offset of P and T waves, we have

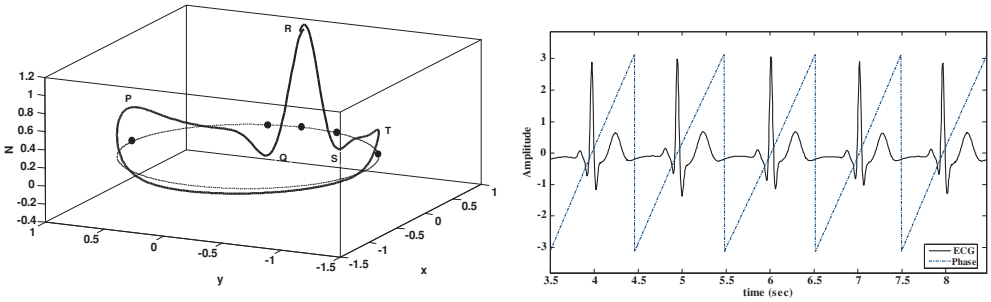

(a) (b)

Figure 2. (a) Typical trajectory generated by the ECG dynamical model (1) in the 3D space given by (x, y, z). The small circles show the center positions of the P, Q, R, S and T events on the limit cycle of unit radius. (b) Typical generated ECG and the corresponding phase signal.

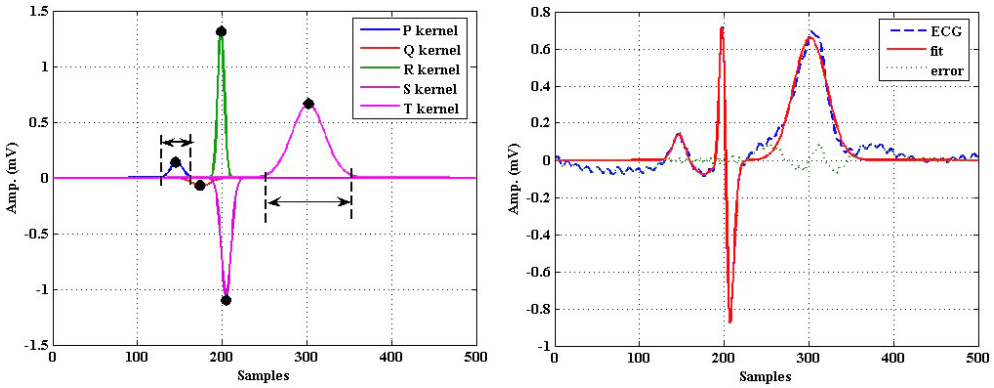

(a) (b)

Figure 3. (a) Five Gaussian functions with arrows indicating the kernels' effect intervals. (b) Real ECG signal and the sum of five Gaussian kernels.

used the approximately 99% confidence bound considering the spread parameters, b_i, for the termination of the two Gaussian functions representing these waves. In other words, when any of the two Gaussian functions representing P and T waves in the dynamical model extends to three times its spread (equal to 99% confidence bound), it is considered as the onset point. The same is true for the offset point. Similarly to detect the *QRS* peaks, we have used the remaining three Gaussian center locations to extract these peaks. To clarify this, refer to figure 3 which declares the above description.

Consequently, the b_i parameter, which corresponds to the σ parameter of a GK, specifies the deviation from the peak position θ_i. This deviation gives the onset and offset points of the PQRST kernels, provided that we assume symmetry for each ECG characteristic waveform. Accordingly, the onset and offset points are given as

$$\begin{aligned} &P_{\text{on}} = \theta_P - 3b_P, && P_{\text{off}} = \theta_P + 3b_P, && QRS_{\text{on}} = \theta_Q - 3b_Q, \\ &QRS_{\text{off}} = \theta_S + 3b_s, && T_{\text{on}} = \theta_T - 3b_T, && T_{\text{off}} = \theta_T + 3b_T. \end{aligned} \tag{4}$$

Having shown the relevance of the Gaussian kernels to the onset and offset points, it is possible to derive analytic expressions for the locations of FPs, based on the estimated state variables. However, when using five Gaussian kernels, the asymmetric properties of some waveforms,

and specially the T wave, may cause errors in determining the wave duration. In other words, more accurate reconstruction is possible if we vary the number of Gaussian functions, as proposed by Clifford *et al* (2005), where asymmetries in waveforms or extra waves (such as the U wave) can be modeled by adding two Gaussians for each asymmetric turning point. Particularly, when six Gaussians are used, the characteristic waveforms are reconstructed almost perfectly, with minimal distortion in the diagnostic information during compression (Sayadi and Shamsollahi 2008a). According to the asymmetric shape of the T wave, for assigning the Gaussians to the PQRST waveforms, two Gaussians are recommended for the T wave, called T+ and T− (Clifford *et al* 2005). This way, distortionless representation of the T wave and especially the ST segment is possible (Sayadi and Shamsollahi 2008a). For the sake of better sensitivity, we insist on using five Gaussians. However, a correction algorithm based on the behavior of the auto-regressive hidden-state variables will be proposed to overcome the errors corresponding to the asymmetric waves.

3. Bayesian framework for estimating the GK parameters

Based on the Gaussian mixture model concept, a mathematical representation for the clean ECG signal can be obtained by integrating the last equation of the continuous form of ECG dynamical model (EDM) introduced in (1) with respect to t (McSharry *et al* 2003). This way, the ECG signal is formulated as a sum of five Gaussians as

$$z(\alpha_i, b_i, \theta_i) = \sum_{i \in \{P,Q,R,S,T\}} \alpha_i \exp\left(-\Delta\theta_i^2 \big/ 2b_i^2\right). \tag{5}$$

The proposal to use the EDM as a basis for estimating the parameters of the mixture model was previously introduced using an optimization scheme to find the least-squares error fit for the input ECG (Clifford *et al* 2005). This fit was mathematically optimal in the LSE sense but did not use any dynamical adaptable information about the input ECG. In the previous approach, the nonlinear optimization has to be performed within each cycle of the signal. Also, initial values of the parameters of the model are required. These initials together with the system dynamics enable us to find an optimal fit for the proceeding cycles through the solution (5). This optimization-based approach was recently adopted for FP extraction from baseline wandered ECG records (Sayadi and Shamsollahi 2008c).

On the other hand, the Bayesian filtering framework showed promising results in ECG denoising (Sameni *et al* 2007) and compression (Sayadi and Shamsollahi 2008a). Accordingly, because the modified framework estimates the parameters of the Gaussian kernels of the EDM (Sayadi and Shamsollahi 2008a), this idea comes to mind that we can extend the SSM for detecting the FPs of an ECG signal. The current approach is also based on the EDM. However, the Bayesian filters use the dynamical set of equations in the construction of an adaptive filter which not only uses the ECG as an observation but also depends on the state dynamics. Furthermore, the EKF-based algorithm does not need to have the initial parameters for every cycle of the input signal. Hence, it seems to be an efficient idea for providing the estimations of GK parameters. In the current study, we have chosen the Bayesian framework, instead of the LSE optimization, to find the estimations of the GK parameters. In this section, we review the modified Bayesian framework proposed by Sayadi and Shamsollahi (2008a) and its application to the estimation of GK parameters.

Sameni *et al* (2007) suggested a nonlinear SSM for representing noisy ECG signals. The idea that long-term ECGs can be described by a series of states described by a given power-spectral density with similar parameters over the short term motivated us to propose autoregressive (AR) dynamics to obtain the modified EDM (Sayadi *et al* 2007, Sayadi and

Shamsollahi 2008a). In this model, the parameters of the Gaussian functions are considered as hidden-state variables with first order AR dynamics and no corresponding observations. This modified model is summarized as follows (Sayadi and Shamsollahi 2008a):

Process equation:

$$\begin{cases} \varphi_{k+1} = \varphi_k + \omega \cdot \delta \\ s_{k+1} = s_k - \sum_{i=1}^{N} \delta \cdot \frac{\alpha_{i_k}\omega}{b_{i_k}^2} \cdot \Delta\theta_i[k] \exp\left(-\frac{\Delta\theta_{i_k}^2}{2b_{i_k}^2}\right) + \eta \\ \alpha_{1_{k+1}} = \alpha_{1_k} + u_{1_k} \\ \vdots \\ b_{1_{k+1}} = b_{1_k} + u_{N+1_k} \\ \vdots \\ \theta_{1_{k+1}} = \theta_{1_k} + u_{2N+1_k} \\ \vdots \\ \theta_{N_{k+1}} = \theta_{N_k} + u_{3N_k}. \end{cases} \tag{6}$$

Observation equation:

$$\begin{cases} \phi_k = \varphi_k + v_k \\ y_k = s_k + w_k, \end{cases} \tag{7}$$

where N is the number of Gaussian kernels. In (6) and (7), φ, s, α_i, b_i and θ_i $(i = 1, \ldots, N)$ are assumed as the state variables, and ω, η and u_j $(j = 1, \ldots, 3N)$ are assumed as i.i.d Gaussian random variables considered as process noises. In the observation equation (7), ϕ and y are the phase observations and the noisy ECG measurements, respectively, and v and w are the corresponding observation noises. The process noise and observation noise vectors of the proposed SSM are defined as follows:

$$\begin{aligned} W &= [\omega, \eta, u_1, \ldots, u_{3N}]^T, \\ V &= [v, w]^T. \end{aligned} \tag{8}$$

All entries of W and V are assumed as zero-mean random variables, with corresponding covariance matrices $Q_k = E\{W_k W_k^T\}$ and $R_k = E\{V_k V_k^T\}$, which incorporate any uncertainty of the SSM (Gelb 1974, Simon 2006).

By defining $x = [\varphi, s, \alpha_1, \ldots, \alpha_N, b_1, \ldots, b_N, \theta_1, \ldots, \theta_N]^T$ as the state vector, and $\hat{x}$ as the posterior estimate of x, the posterior error of the estimation at the time instant k is defined as $e_k = x_k - \hat{x}_k$ with a covariance matrix $P_k = E\{e_k e_k^T\}$. The matrix P_k is an essential part of the standard Kalman filter (KF) and is calculated and updated as the filter propagates in time.

The modified dynamic model proposed in (6) is a nonlinear function of the state and process noise vectors. Therefore, nonlinear extensions of the KF are required for estimating the state vector x. Our proposed framework is built upon an EKF structure. Although there are several Bayesian filters such as the extended Kalman smoother (EKS) and unscented Kalman filter (UKF), in this research, we have chosen the EKF for its simplicity and more numerical stability. However, the overall filtering performance is expected to be better with EKS or UKF (Sameni *et al* 2007).

In order to implement the EKF, the time propagation and the measurement propagation equations are summarized as follows (Kay 1981):

$$\begin{cases} \underline{\hat{x}}_{k+1}^{-} = f(\underline{\hat{x}}_k^{+}, \underline{w}, k)|_{\underline{w}=\underline{0}} \\ P_{k+1}^{-} = A_k P_k^{+} A_k^T + F_k Q_k F_k^T, \end{cases}$$
$$\begin{cases} \underline{\hat{x}}_k^{+} = \underline{\hat{x}}_k^{-} + K_k[\underline{y}_k - g(\underline{\hat{x}}_k^{-}, \underline{v}, k)|_{\underline{v}=\underline{0}}] \\ K_k = P_k^{-} C_k^T [C_k P_k^{-} C_k^T + G_k R_k G_k^T]^{-1} \\ P_k^{+} = P_k^{-} - K_k C_k P_k^{-}, \end{cases} \tag{9}$$

where

$$\begin{aligned} A_k &= \left.\frac{\partial f(\underline{x}, \underline{\hat{w}}_k, k)}{\partial \underline{x}}\right|_{\underline{x}=\underline{\hat{x}}_k} & F_k &= \left.\frac{\partial f(\underline{\hat{x}}_k, \underline{w}, k)}{\partial \underline{w}}\right|_{\underline{w}=\underline{\hat{w}}_k} \\ C_k &= \left.\frac{\partial g(\underline{x}, \underline{\hat{v}}_k, k)}{\partial \underline{x}}\right|_{\underline{x}=\underline{\hat{x}}_k} & G_k &= \left.\frac{\partial g(\underline{\hat{x}}_k, \underline{v}, k)}{\partial \underline{v}}\right|_{\underline{v}=\underline{\hat{v}}_k}. \end{aligned} \tag{10}$$

In the above EKF formulation, f and g stand for the process functions (6) and observation functions (7), respectively. Suppose that the EKF is applied to an ECG signal, based on the modified dynamical system (6). The provided estimations are a set of $(3 \times N + 2)$ state variables, whose estimate is in the form of a time series. The time series include the following.

(i) *Estimation of the phase signal* ($\hat{\varphi}$). This estimation is expected to resemble a saw-tooth-shape signal with phase assignments between $-\pi$ and π to the ECG samples between two successive R-peaks.

(ii) *Estimation of the ECG signal* ($\hat{s}$). This estimation is provided by summation of N Gaussian kernels, as shown in (1). Each Gaussian function has three parameters; amplitude (α_i), center (θ_i) and spread (b_i), which control the fitness of the kernels to the waveforms of the ECG signal.

(iii) *Estimation of the amplitudes of Gaussian kernels* ($\hat{\alpha}_i$). These N hidden-state variables determines the amount of offset needed to push the circular limit cycle, up and down, as it approaches each Gaussian center. In particular, for $N = 5$, the amplitude estimations correspond directly to the amplitudes of five main ECG waveforms, i.e. P, Q, R, S and T. For a monotonic ECG, in which successive beats follow a similar morphology, it is expected that the amplitudes of the waveforms remain almost unchanged during successive cycles (Sayadi and Shamsollahi 2008a).

(iv) *Estimation of the center of Gaussian kernels* ($\hat{\theta}_i$). These estimations determine the local maximum or the minimum of the trajectory, with respect to the wrapped phase $\Delta\theta_i$. Although there exist negligible variations in different beats, the centers are expected to appear in same locations on the wrapped limit cycle, during successive heartbeats.

(v) *Estimation of the spread of Gaussian kernels* ($\hat{b}_i$). These estimations determine the width of each Gaussian function and correspond to the temporal spread of each kernel around its center. Again, it is expected that the width of each kernel remains almost unchanged. This is implied from the auto-regressive dynamics introduced in (6).

Accordingly, the first- and second- state variables give the phase and ECG signal estimations. Other state variables give estimations of the parameters of N Gaussian functions. In order to obtain the segment symbols, it is now reasonable to assign the parameters of these kernels to the temporal locations of the FPs, according to (3) and (4).

4. The correction algorithm

To investigate the functionality of the proposed EKF structure in correcting the determination of the FPs, first, we should study the role of autoregressive equations. The dynamical state-space

model (6) implies that the 3rd to $(3N + 2)$th state variables are the parameters of N Gaussian kernels. In order to ensure a valid set of equations, and because the Gaussian parameters are expected to have little variations from one beat to another beat in monotonic ECG signals, only one term is added to the previously estimated value to obtain current estimation at instant $k + 1$. In other words, we expect that the recent sample can be regressed on the past value of itself. This concept can be narrated in a simpler manner, in order to relate the EKF framework to the beat segmentation problem.

Suppose a general first-order auto-regressive model, namely AR[1], is shown as follows:

$$z_{k+1} = \gamma z_k + u_k, \tag{11}$$

where γ is the model coefficient and u is a zero mean white process noise. If we want to estimate the best model for a given time series, then the AR coefficient γ can be estimated from the autocorrelation sequence by solving the Yule–Walker equations. Based on this concept, it is expected that the hidden state variables show a quasi-constant behavior. Since the hidden variables are the parameters of the Gaussian kernels of the EDM, they are estimated in such a way to result in the best fit to the Gaussian mixture model dynamics. This way, the filter encounters two types of observation samples.

(i) *In-kernel samples*. Parts of the observation signal y that form any of the P, Q, R, S and T waveforms are called *in-kernel* for the ith Gaussian kernel, if they correspond to α_i, b_i and θ_i variables.
(ii) *Out-kernel samples*. Parts of the observation signal y that do not belong to PQRST, or parts that are in kernel of the ith Gaussian function, but correspond to α_j, b_j and $\theta_j (j \neq i)$ are called *out-kernel*.

For example, consider the case that the ECG signal is modeled with five kernels. The samples of P waves in the ECG signal are in-kernel for the first Gaussian function, that relates the observation to α_1, b_1 and θ_1, and out-kernel for the remaining Gaussian functions, that is α_j, b_j and $\theta_j (j \neq 1)$. Similarly, the samples of Q waves are in-kernel for the second Gaussian function, while out-kernel for the first, third, fourth and fifth Gaussian functions. This classification is the key through behavior analysis of estimated variables.

When the filter encounters an in-kernel sample, it tries to find the best estimate of the hidden variables according to the AR[1] dynamics. On the other hand, the corresponding ECG waveform has not end up in this sample. Hence, the estimate uses the previous observation samples and is not capable of performing a reliable estimation for the mentioned sample. The unreliable estimation continues, unless the waveform ends up, corresponding to the beginning of the introduction of the first out-kernel sample to the filter. At this location, the filter provides a reliable estimation, leading to a quasi-constant behavior.

According to the above description, it is reasonable to expect a fluctuation in the estimated time series of the in-kernel samples, while a quasi-constant behavior is expected for the out-kernel samples. On the other hand, in-kernel samples point to the duration of each waveform. Thus, the fluctuating parts of the estimations provided by the EKF structure show an estimation of the waveform bounds (Sayadi and Shamsollahi 2008b).

Combining the approach discussed in section 3.1 with the correction algorithm, which is based on the fluctuations in the estimated Gaussian parameters, the following formula is given to determine the onset and offset points of the ECG waveforms:

$$\begin{aligned}
P_{\text{on}} &= \min\left(\theta_P - 3b_P, f_P^{\text{on}}\right) & P_{\text{off}} &= \max\left(\theta_P + 3b_P, f_P^{\text{off}}\right) \\
QRS_{on} &= \min\left(\theta_Q - 3b_Q, f_Q^{on}\right) & QRS_{\text{off}} &= \max\left(\theta_S + 3b_s, f_S^{\text{off}}\right) \\
T_{\text{on}} &= \min\left(\theta_T - 3b_T, f_T^{\text{on}}\right) & T_{\text{off}} &= \max\left(\theta_T + 3b_T, f_T^{\text{off}}\right),
\end{aligned} \tag{12}$$

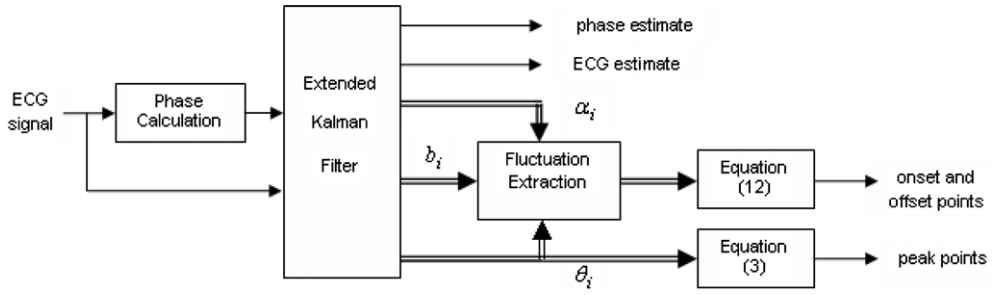

Figure 4. General block diagram for the proposed segmentation algorithm.

Table 1. Rule chart for the extraction of ECG morphological features using the Gaussian kernel parameters.

Feature	Relevance to the fiducial points	Extraction formula
P_{amp}	Amplitude of the ECG signal at P_{peak}	α_p
QRS^{-}_{amp}	Minimum amplitude of the ECG signal at Q_{peak}, R_{peak}, S_{peak}	$\min(\alpha_Q, \alpha_R, \alpha_S)$
QRS^{+}_{amp}	Maximum amplitude of the ECG signal at Q_{peak}, R_{peak}, S_{peak}	$\max(\alpha_Q, \alpha_R, \alpha_S)$
T_{amp}	Amplitude of the ECG signal at P_{peak}	α_T
P_{dur}	Difference between the onset and offset of the P wave	$P_{\text{off}} - P_{\text{on}}$
QRS_{dur}	Difference between the onset of the Q wave and offset of the S wave	$S_{\text{off}} - Q_{\text{on}}$
T_{dur}	Difference between the onset and offset of the T wave	$T_{\text{off}} - T_{\text{on}}$
RR_{int}	Difference between the peak locations of two successive R waves	$R'_{\text{peak}} - R_{\text{peak}}$
QT^{p}_{int}	Difference between peak locations of the Q wave and T wave	$T_{\text{peak}} - Q_{\text{peak}}$
QT_{int}	Difference between the peak location of the Q wave and offset of T wave	$T_{\text{off}} - Q_{\text{peak}}$
TP_{int}	Difference between the peak locations of the T wave and next P wave	$P'_{\text{peak}} - T_{\text{peak}}$

where f_i^{on} and f_i^{off} stand for the onset and offset of the fluctuating part of waveform i, which are detected based on the zero-crossings of slope changes in the estimated signal. Here, the slope signal is constructed using the first or the second derivative, or equivalently one can use the slope signal introduced by Lee *et al* (2005) as

$$\text{slope}_k = 2g_{k+2} + g_{k+1} - g_{k-1} - 2g_{k-2}, \tag{13}$$

where g is the Gaussian kernel parameters α_i, b_i and θ_i. The overall beat segmentation algorithm is illustrated in figure 4. It is worthy to note that all of the morphological features can be written in the form of these notations, which are summarized in table 1.

5. Simulation results

The proposed algorithm was implemented in MATLAB®. The MIT-BIH Normal Sinus Rhythm Database (Goldberger *et al* 2000, MIT-BIH Normal Sinus Rhythm Database 1991) was used to study the performance of the proposed method. This database has a sampling rate of 128 Hz. From this database, 80 low-noise segments of 30 s ECG without considerable artifacts were visually selected from different channels. The manual detection was used to provide a known reference for the exploration, so these ECGs were first annotated completely by experienced cardiologists from Tehran Heart Center (THC).

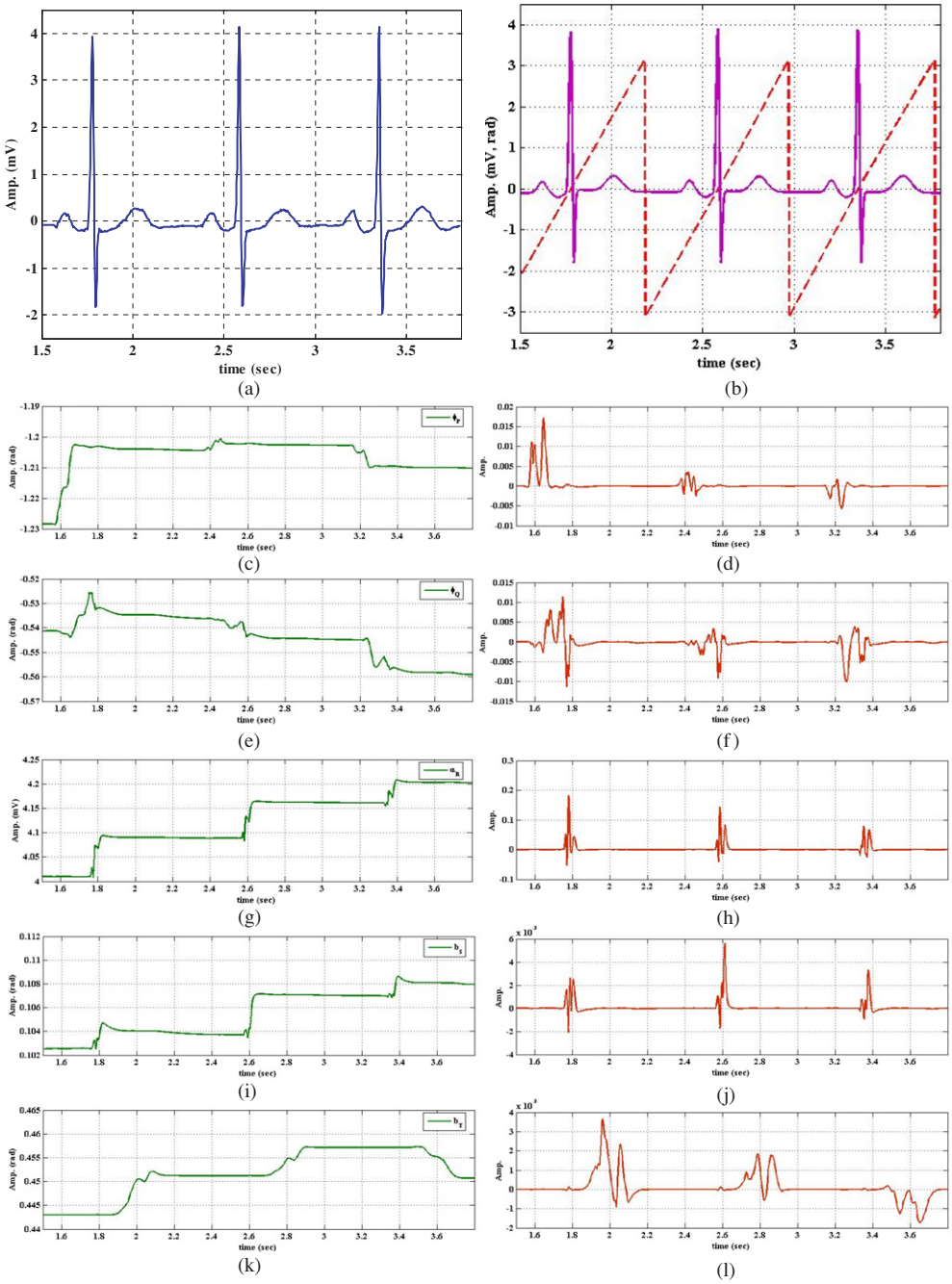

Figure 5. Typical estimated state variables for an ECG signal. (a) Input signal, (b) phase and ECG estimations, (c) θ_P, (d) slope of θ_P, (e) θ_Q, (f) slope of θ_Q, (g) α_R, (h) slope of α_R, (i) b_S, (j) slope of b_S, (k) b_T and (l) slope of b_T.

Figure 5 shows an ECG signal, typical state variable estimates and the corresponding slope signals. It can be seen that the fluctuations correspond to the in-kernel samples, which determine the duration of each waveform by zero-crossing detection of the slope signals.

Table 2. Performance evaluation of the proposed method for segment symbol extraction using sensitivity (Sn), specificity (Sp) and positive predictivity (+P). The number of true recognitions (true positive, TP, and true negative, TN, detections) together with the number of false recognitions (false positive, FP, and false negative, FN, detections) are provided with/without using the correction algorithm.

Measure	Correction algorithm	Record number					Total
		16265	16272	16273	16420	16483	
TP	No	6683	4669	5055	6540	5903	28 850
	Yes	7744	5104	6160	7392	8096	34 496
TN	No	82 357	54 218	65 501	78 593	86 012	366 681
	Yes	82 357	54 218	65 501	78 593	86 012	366 681
FP	No	1087	438	1116	852	2212	5705
	Yes	26	3	11	0	19	59
FN	No	0	0	0	0	0	0
	Yes	0	0	0	0	0	0
Sn (%)	No	100	100	100	100	100	100
	Yes	100	100	100	100	100	100
Sp (%)	No	97.97	99.20	98.32	98.93	97.49	98.47
	Yes	99.96	99.94	99.82	100	99.76	99.83
+P (%)	No	86.01	91.42	81.92	88.47	72.74	83.49
	Yes	99.97	99.99	99.98	100	99.98	99.98

Prior to the implementation of the proposed method, it is necessary to select the initial value for the state vector as well as the selection of the covariance matrices of the process and the measurement noise, which will influence the trajectory of the estimated vectors. The interested reader is referred to Sameni *et al* (2007), where an efficient automated selection procedure for any given ECG was used. In this study, we have used the same procedure as Sayadi and Shamsollahi (2008a) for the initialization of the modified EKF structure.

In order to evaluate the performance of the proposed beat segmentation technique, we have used the following parameters to evaluate our method: number of true positive detections (TP), number of false positive detections (FP), number of true negative detections (TN) and number of false negative detections (FN). Obviously, TP and TN show the correct points' recognition by the algorithm. Hence, it is expected that TP equals the number of all FPs, and TN equals the number of all non-FPs. According to the above terminology, sensitivity (Sn), specificity (Sp) and positive predictivity (+P) criteria are defined as

$$\mathrm{Sn} = \frac{TP}{TP + FN}, \tag{14}$$

$$\mathrm{Sp} = \frac{TN}{TN + FP}, \tag{15}$$

$$+\mathrm{P} = \frac{TP}{TP + FP}. \tag{16}$$

Performance evaluation results are provided for all of the 80 ECG segments, chosen from five channel recordings of approximately 8 min long. Table 2 shows the results for two different approaches: the FP detection using equation (4) where no correction algorithm is being applied, and using equation (12) which is based on the correction algorithm.

It can be seen that the correction algorithm improves the point extraction results greatly. Specifically, for records with asymmetric waveforms, the fluctuation parts of the estimations

Table 3. Performance evaluation of benchmark methods for ECG components detection and comparison to the proposed model-based method.

	Benchmark methods[a]			Proposed method		
Components	Sn (%)	Sp (%)	+P (%)	Sn (%)	Sp (%)	+P (%)
P wave	90.24	91.08	84.18	100	98.76	99.11
QRS complex	98.79	99.91	99.90	100	99.93	99.96
T wave	95.32	98.80	99.25	100	99.06	99.39

[a] Benchmark methods include Gritzali *et al* (1989) for P and T wave detection, and Li *et al* (1995) for QRS detection.

provided by the EKF play the major role in min–max operations (12). Hence, the enhancement is much more obvious for these cases. Particularly, the decrease in the FP detections yields very satisfactory positive predictivity ratios (99.98%) compared to the results using (4) where no correction algorithm is applied (83.49%).

As mentioned before, we have restricted the EDM to model a single ECG cycle as the summation of five Gaussian kernels. Although $N = 5$ is not sufficient to incorporate the diagnostic specifications and the asymmetric properties of ECG signals, particularly in compression applications (Sayadi and Shamsollahi 2008a), but it is beneficial for having no FN detections. In other words, the model with five Gaussian functions is limited to give 15 kernel parameters, which are estimated through the EKF structure. These parameters specify the GMM for any cycles of the signal, which match to PQRST waveforms. Hence, no extra false points are detected. Accordingly, the sensitivity of the method for all of the records is always 100%, independent of applying the correction algorithm. This is beneficial especially for ECGs containing ambiguous waves. Furthermore, the specificity and positive predictivity results are well within the acceptable range. It can be seen that none of the analyzed cases result in specificity less than 99.66% and positive predictivity of 99.97%.

There are few works which focus on determining all the FPs of an ECG. The majority of these include feature extraction approaches for classification, or compression evaluation. Here, we can obtain all of the features relating to locations (6) and (8) or time intervals, listed in table 1. However, to investigate the validity of the results, we have compared the model-based algorithm to some of the benchmark methods for ECG characteristic wave extraction. Numerical evaluation results are reported in table 3. It can be seen from table 3 that our proposed method provides a higher specificity and positive predictivity, while preserving the zero false-negative detection. Additionally, for all components, the results of our algorithm is comparable to and usually superior to the other methods being tested, which shows the ability of the proposed framework to detect the P and T waves and the QRS complex. Hence, the model-based algorithm extracts the characteristic components of the signal more accurately.

As a graphical representation, it is time to show typical locations of the FPs on some ECG signals. Figure 6 shows the results of applying the proposed segmentation algorithm on two different ECG records. As can be seen, the distinguished precise FPs indicated by circles are clearly at their exact locations, compared to the manual detection results. To appreciate the merits of the proposed algorithm, and to show the consistency of the results to the manual detections, we have shown the distinguished FPs by an expert, as well as the detections of the proposed algorithm and some benchmark methods, all in figure 7. The ECG record contains low amplitude P waves with inverted T waves. A simple visual comparison shows the capability of the Bayesian framework, compared to the benchmark methods, especially for detecting the onset and offset of P waves which pertain to be biphasic, and also asymmetric T waves.

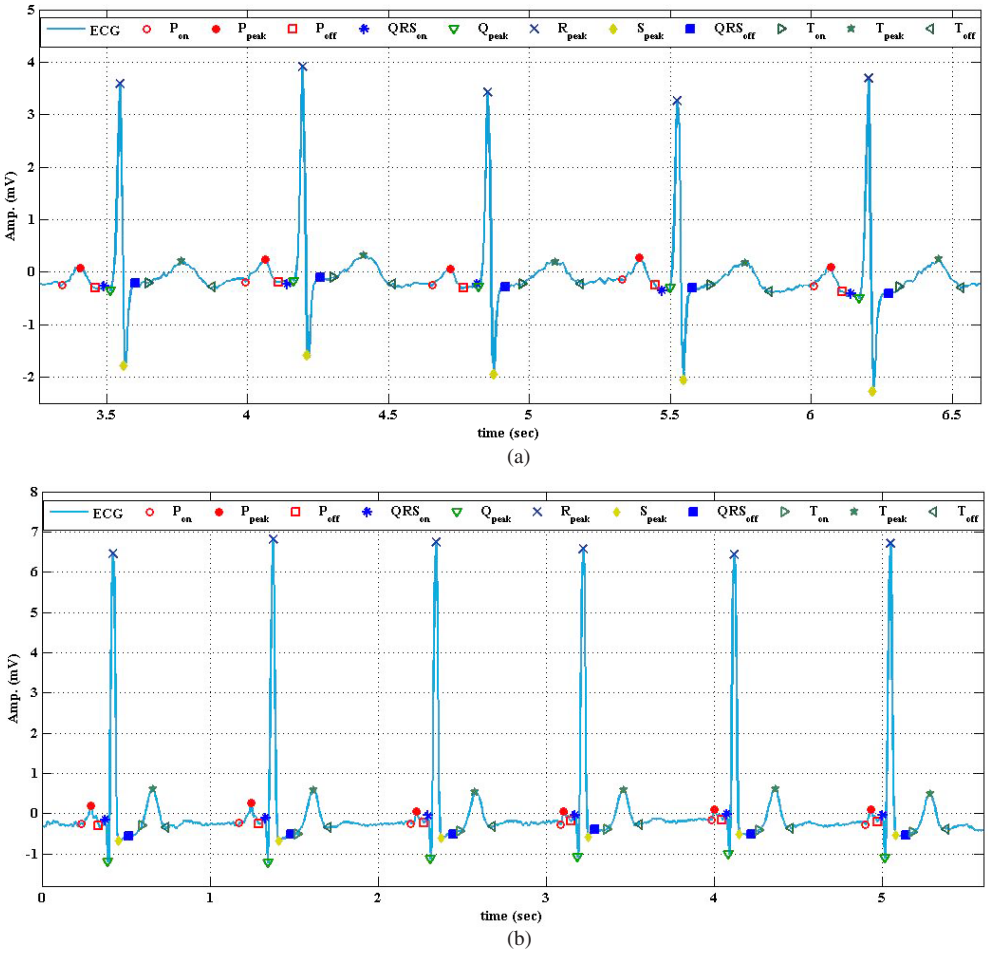

Figure 6. Segmentation results for two typical ECG signals. (a) Fiducial points for record no. 16420, (b) fiducial points for record no. 16273.

In order to investigate the segmentation results of the proposed model-based algorithm statistically, histograms of deviations between the markings of the automatic algorithm compared to the 'gold standard' of manually measured P wave duration, QRS duration, QT intervals and TP intervals are presented in figure 8.

The deviations of the method are much better compared to the results obtained with recent benchmark methods (Meyer *et al* (2006) for QRS duration, Portet (2008) for P wave duration, Christov and Simova (2007) for QT interval). The figures demonstrate that the deviations behave like a normal distribution for those detections which rely on peak points, i.e. $\mathrm{QRS}_{\mathrm{dur}}$ and $\mathrm{TP}_{\mathrm{int}}$, which are calculated using (4). Moreover, for these cases, the error is not considerable (mostly below 10 ms). However, the segmentation results for P_{dur} and QT_{int} are very similar to log-normal distributions, which is as the result of the asymmetric detection properties of (12). Similar to the previous cases, the deviations are well in the acceptable range (below 50 ms), even facing common difficulties such as the noise accompanying the ECGs, the low magnitude of the T wave, T having bidirectional waveform, fussing U waves, etc. It can definitely be said that the proposed automated method possess acceptable accuracy

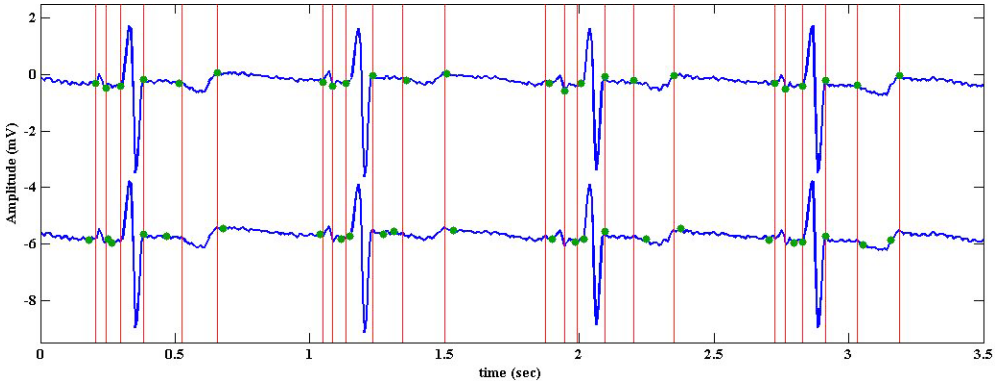

Figure 7. Segmentation results for a typical ECG signal, including the onset and offset of P, QRS and T waves. The vertical lines show the manual detection results by expert. The upper plot shows the results of the proposed algorithm, and the lower plot shows the results of benchmark-automated methods (Gritzali *et al* 1989, for P and T waves detection, and Li *et al* 1995, for QRS detection).

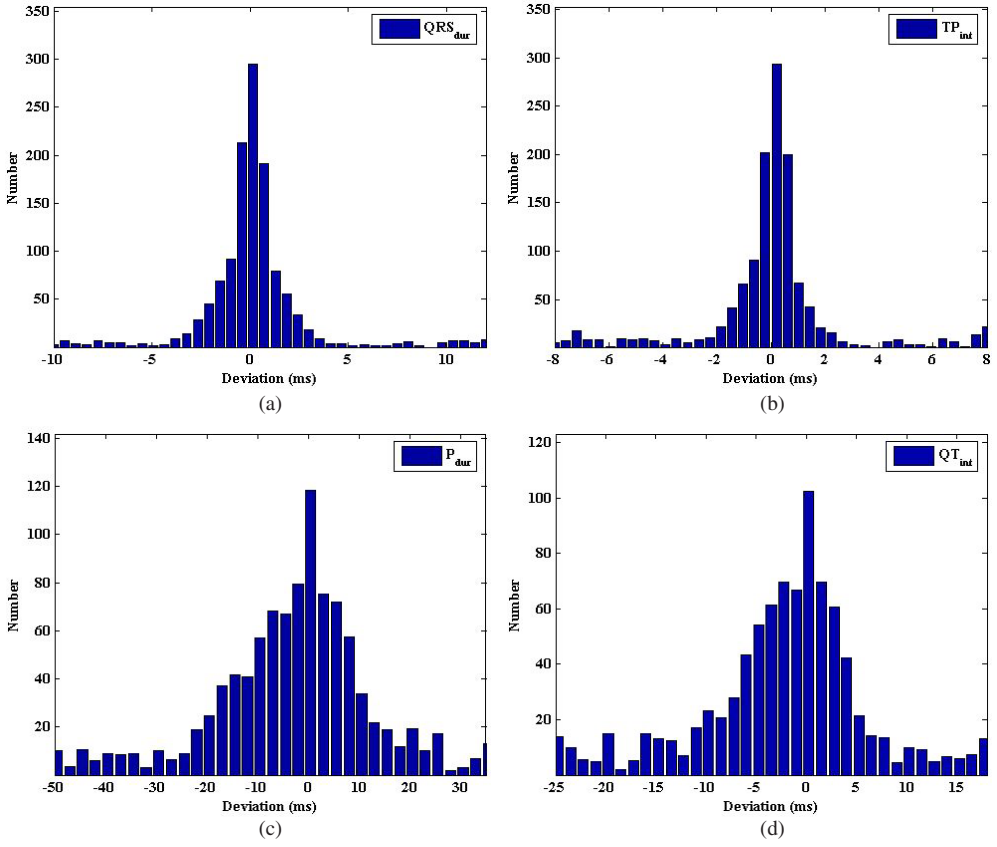

Figure 8. Histograms of deviations between the markings of the proposed automatic algorithm compared to the 'gold standard' of manually measured indices including (a) QRS duration, (b) TP interval, (c) P wave duration and (d) QT interval.

for clinical evaluations. Furthermore, combining the tracking properties of the EKF structure with the model-based idea, accuracy close to the experts' measurements can be obtained.

Another important issue is the limited range of deviations and their relation to the sampling frequency of the records. Figure 8 implies that the deviation lies in the interval of $[-10, 12]$ ms for peak detections and $[-50, 38]$ ms for interval extraction. Since the sampling frequency is 128 Hz, the former corresponds to 1 or 2 sample difference, and the latter corresponds to maximum 7 samples deviation from the manually located points. However, it was shown that for higher sampling frequencies (such as 360 Hz), the error is expected to be fewer than the above results (Sayadi and Shamsollahi 2008b).

6. Discussion and conclusion

In this paper, a model-based Bayesian framework was presented and validated for ECG beat segmentation. The method is based on a modified EKF algorithm that incorporates the parameters of the ECG dynamical model. By introducing a simple AR model for each of the 15 dynamic parameters of the Gaussians, the new EKF structure was constructed. The proposed set of equations aims at integrating into the ECG model a mechanism that estimates the new hidden-state variables without having any corresponding observations, which was later used for analytic FP extraction. The designed filter was applied to various ECG signals, and the results demonstrate the filter's capability in filtering and tracking the parameters of a GMM for the ECG signal.

The EKF structure not only estimates the clean ECG as a Kalman state variable, but also estimates the Gaussians parameters of the model. Therefore, a formula was derived to match the parameters of Gaussian kernels to the locations of the FPs. This presents the greatest potential of the presented mathematical model-based framework, with which the morphology is tracked efficiently. We also derived rules to locate the peaks of characteristic waves, based on the estimated state variables. Moreover, investigation of the AR dynamics paved the way toward the fluctuation concept, which was further used to correct the FP analytic derivation.

From a filtering point of view, KFs can be assumed as adaptive filters that continuously move the location of the poles and zeros of their transfer functions, according to the signal or noise content of the input observations and the prior model of the signal dynamics. This way, we can be sure of the reliability of the estimations, resulting in precise FP extraction and beat segmentation. Moreover, this feature allows the filter to adapt with different spectral shapes and temporal non-stationarities, since the variance of the observation noise in (2) represents the degree of reliability of a single observation, as well as the degree of adaptively tracking the input noisy measurement. However, in the context of FP extraction, the reliability on the measurements is not of any interest.

The method was validated using several ECG recordings, including lead II and V2, in which the PQRST waveforms are dominant. Although the dynamical model is able to adapt to various morphologies of other leads, attentions should be paid to the definitions of the FPs for non-standard ECGs, such as those records in which some waveforms are occasionally missing and the QRS complex is not in the standard form. It is worth noting that the initial value for the state vector as well as the selection of the covariance matrices of the process and the measurement noise will highly influence the trajectory of the estimated vectors. The dependence of the results on these initials is the major drawback of the proposed method.

Performance evaluation results showed that the developed method provides a reliable and accurate detection of the FPs, providing a mean specificity of 99.83% and a mean positive predictivity of 99.98%, which is well within the acceptable range. In addition, by selecting five Gaussian kernels, the false negative ratio was reduced to zero, which resulted in sensitivity

of 100% for all cases. Moreover, in comparison to other proposed methods for components detection, the model-based approach has a superior performance, for there is no decision rules based on comparison against thresholds. It was also shown that the proposed method is applicable to reliable P wave and T wave detection. Particularly, the performance of the system is expected to be improved with the increase in the sampling frequency. However, for low-resolution recordings, the deviations remain in an acceptable range.

Due to the recursive structure of the KF, the proposed method is also computationally efficient and of special interest for real-time applications. Generally, the computation time of this method is linearly proportional to the signal length in samples. For the currently developed MATLAB® source codes, the computation time is already close to real time. However, these codes may be further optimized and converted into low-level languages for use in pre-processing units of clinical monitoring systems.

In addition, through simple modifications, the method would be robust to PQRST variations, which incorporates several pathological conditions. Moreover, the adaptive nature of the KF framework results in efficient signal tracking, which is beneficial in generalization of the method for signals with unknown or ambiguous waves.

For the sake of brevity, the presented results were only based on the EKF. However, other types of Bayesian filters such as the UKF and the particle filter (PF) can be used in the same manner for highly nonlinear and non-Gaussian noise scenarios (Haykin 2001).

Future works include incorporating baseline fluctuations in the EDM to reduce the distortions and cause the algorithm to be more reliable. In addition, different dynamical models may be proposed to represent the new state variables' behavior. Also, it is possible not to use a constant value for the AR coefficient but to find an adaptive value during different cycles.

Acknowledgments

We wish to thank Dr A M Hajizeinali and Dr A Yaminisharif, who have shared their expertise in electrocardiography. We are particularly grateful to Dr S Sadeghian for providing detailed answers to our many questions, for his valuable comments and knowledge of the problem. We would also like to thank the Tehran Heart Center (THC) for their cooperation.

References

Afonso V X, Tompkins W J, Nguyen T Q and Luo S 1999 ECG beat detection using filter banks *IEEE Trans. Biomed. Eng.* **46** 192–202

Andreão R V, Dorizzi B, Cortez P C and Mota J C M 2002 Efficient ECG multilevel wavelet classification through neural network dimensionality reduction *Proc. IEEE Workshop on Neural Network for Signal Processing (Martigny, Suisse)* 395–404

Bortolan G, Degani R and Willems J L 1990 Neural networks for ECG classification *Proc. Computers in Cardiology (Chicago, IL)* 269–72

Christov I and Simova I 2007 Q-onset and T-end delineation: assessment of the performance of an automated method with the use of a reference database *Physiol. Meas.* **28** 213–21

Clifford G D, Azuaje F and McSharry P E 2006 *Advanced Methods and Tools for ECG Data Analysis* (Boston: Artech House)

Clifford G D, Shoeb A, McSharry P E and Janz B A 2005 Model-based filtering, compression and classification of the ECG *Int. J. Bioelectromagn.* **7** 158–61

Coast D A, Stern R M, Cano G G and Briller S A 1990 An approach to cardiac arrhythmia analysis using hidden Markov model *IEEE Trans. Biomed. Eng.* **37** 826–36

Elghazzawi Z and Gehed F 1996 A knowledge-based system for arrhythmia detection *Proc. Computers in Cardiology (Indianapolis, IN)* 541–4

Gelb A 1974 *Applied Optimal Estimation* (Cambridge, MA: MIT Press)

Goldberger A L, Amaral L A N, Glass L, Hausdorff J M, Ivanov P C, Mark R G, Mietus J E, Moody G B, Peng C K and Stanley H E 2000 PhysioBank, PhysioToolkit, and PhysioNet: components of a new research resource for complex physiologic signals *Circulation* **101** e215–20 (*Circulation* electronic pages http://circ.ahajournals.org/cgi/content/full/101/23/e215)

Gritzali F, Frangakis G and Papakonstantinou G 1989 Detection of the P and T waves in an ECG *Comput. Biomed. Res.* **22** 83-91

Haykin S 2001 *Kalman Filtering and Neural Networks* (New York: Wiley)

Hu Y H, Palreddy S and Tompkins W J 1997 A patient-adaptable ECG beat classifier using a mixture of experts approach *IEEE Trans. Biomed. Eng.* **44** 891–900

Kadambe S, Murray R and Boudreaux-Bartels G 1999 Wavelet transform-based QRS complex detector *IEEE Trans. Biomed. Eng.* **46** 838–48

Kadish A 2001 ACC/AHA clinical competence statement on electrocardiography and ambulatory electrocardiography *Circulation* **104** 3169–78

Kay S M 1981 Efficient generation of colored noise *Proc. IEEE* **69** 480–1

Krimi S, Ouni K and Ellouze N 2006 T-wave detection based on an adjusted wavelet transform modulus maxima *Int. J. Biomed. Sci.* **1** 128–32

Köhler B U, Hening C and Orglmeister R 2002 The principles of software QRS detection *IEEE Eng. Med. Biol. Mag.* **21** 42–57

Kors J A and Van Bemmel J H 1990 Classification methods for computerized interpretation of the electrocardiogram *Methods Inf. Med.* **29** 330–6

Laguna P, Jané R and Caminal P 1994 Automatic detection of wave boundaries in multilead ECG signals. Validation with the CSE database *Comput. Biomed. Res.* **27** 45–60

Lee R G, Cho1 I C, Lai C C, Liu M H and Chiu M J 2005 A novel QRS detection algorithm applied to the analysis for heart rate variability of patients with sleep apnea *J. Biomed. Eng. Appl. Basis Commun.* **17** 258–62

Li C, Zheng C and Tai C 1995 Detection of ECG characteristic points using wavelet transforms *IEEE Trans. Biomed. Eng.* **42** 21–8

Mahmoodabadi S Z, Ahmadian A and Abolhasani M D 2005 ECG feature extraction using Daubechies wavelets *Proc. IASTED (Benidorm, Spain)* 343–8

McSharry P E, Clifford G D, Tarassenko L and Smith L A 2003 A dynamic model for generating synthetic electrocardiogram signals *IEEE Trans. Biomed. Eng.* **50** 289–94

Meyer C, Gavela J F and Harris M 2006 Combining algorithms in automatic detection of QRS complexes in ECG signals *IEEE Trans. Inf. Tech. Biomed.* **10** 468–75

MIT-BIH Normal Sinus Rhythm Database 1991 (http://www.physionet.org/physiobank/database/nsrdb/)

Portet F 2008 P wave detector with PP rhythm tracking: evaluation in different arrhythmia contexts *Physiol. Meas.* **29** 141–55

Sameni R, Shamsollahi M B and Jutten C 2008 Model-based Bayesian filtering of cardiac contaminants from biomedical recordings *Physiol. Meas.* **29** 595–613

Sameni R, Shamsollahi M B, Jutten C and Clifford G D 2007 A nonlinear Bayesian filtering framework for ECG denoising *IEEE Trans. Biomed. Eng.* **54** 2172–85

Sayadi O, Sameni R and Shamsollahi M B 2007 ECG denoising using parameters of ECG dynamical model as the states of an extended Kalman filter *Proc. EMBC '07 (Lyon, France)* pp 2548–51

Sayadi O and Shamsollahi M B 2008a ECG denoising and compression using a modified extended Kalman filter structure *IEEE Trans. Biomed. Eng.* **55** 2240–8

Sayadi O and Shamsollahi M B 2008b Model-based ECG fiducial points extraction using a modified extended Kalman filter structure *Invited paper ISABEL '08 (Aalborg, Denmark)* pp 1–5

Sayadi O and Shamsollahi M B 2008c Model-based fiducial points extraction for baseline wandered electrocardiograms *IEEE Trans. Biomed. Eng.* **55** 347–51

Simon D 2006 *Optimal State Estimation* (New York: Wiley)

Skordalakis E 1986 Syntactic ECG processing: a review *Pattern Recog.* **19** 305–13

Vullings H J L M, Verhaegen M H G and Verbruggen H B 1998 Automated ECG segmentation with dynamic time warping *Proc. EMBC '98 (Hong Kong)* pp 163–6